PROCEEDINGS OF SCIENCE

ONLINE ICRC 2021
THE ASTROPARTICLE PHYSICS CONFERENCE
Berlin | Germany
37th International Cosmic Ray Conference
12–23 July 2021

On-orbit energy calibration of the calorimeter on the ISS-CREAM instrument using the boronated scintillator detector

Yu Chen,[a,*] **Tyler Anderson,**[a] **Stephane Coutu,**[a] **Tyler LaBree,**[b] **Jason T. Link,**[c,d] **John W. Mitchell,**[d] **S.A. Isaac Mognet,**[a] **Scott L. Nutter,**[b] **Kenichi Sakai,**[c,d] **Jacob Smith**[c,d] **and Monong Yu**[a]

[a] *Penn State University, Department of Physics, University Park, PA, 16802, USA*
[b] *Northern Kentucky University, Dept of Physics, Geology, and Engineering Technology, Highland Heights, KY, 41099, USA*
[c] *Center for Research and Exploration in Space Science and Technology (CRESST), UMBC, Baltimore MD, 21250, USA*
[d] *NASA Goddard Space Flight Center, Astroparticle Physics Laboratory, Greenbelt, MD, 20771, USA*
E-mail: yuc357@psu.edu

The Cosmic Ray Energetics And Mass instrument on the International Space Station (ISS-CREAM) aims to measure the energy spectra of cosmic ray (CR) nuclei from Z=1 to Z=26 with energies from 10^{12} eV to 10^{15} eV. The calorimeter (CAL) was designed to measure the energy of the CR particles. The ISS-CREAM on-orbit data provide evidence that the CAL may have either suffered from an efficiency problem or its energy scale may be in need of calibration. As a result, a careful scrutiny of the absolute energy calibration of the CAL is required. We describe an approach to calibrate the energy scale using the on-orbit data of the boronated scintillator detector, which is independent of the CAL data and reduces potential bias. We discuss the issues revealed by the on-orbit data, demonstrate how this can be corrected using the boronated scintillator detector and present preliminary results.

37th International Cosmic Ray Conference (ICRC 2021)
July 12th – 23rd, 2021
Online – Berlin, Germany

*Presenter

PoS(ICRC2021)074

1. Introduction

The acceleration and propagation of cosmic rays remain open questions and active fields of inquiry, over a century after their discovery. In particular, the elucidation of spectral features such as the knee (3×10^{15} eV) is crucial in constraining models of their Galactic origin and transport [1]. This knee energy regime was once out of reach of the traditional balloon-based instruments given their limited acceptance and balloon exposures. The situation has changed with the launch of space-based cosmic ray detectors, such as AMS-02 [2], CALET [3], DAMPE [4]. The Cosmic Ray Energetics And Mass Instrument on the ISS (ISS-CREAM) is the successor of the previous balloon-based CREAM experiment and also aims to push the direct measurement of CRs to the knee region. ISS-CREAM was launched and deployed on the Japanese Experiment Module (Kibo) of the ISS in August, 2017 and operated until February, 2019.

2. Analyzing the ISS-CREAM data

2.1 The ISS-CREAM instrument

ISS-CREAM consists of several sub-detectors and each measures different aspects of the CR particle. The Silicon Charge Detector (SCD) [5] determines the charge with a resolution of $0.1 - 0.3e$. The Top and Bottom Counting Detectors (TCD and BCD) [6] are designed to distinguish electrons from protons and to provide an instrument trigger. For the energy measurement, ISS-CREAM uses a densified graphite block, which is equivalent to 0.5 nuclear interaction length, to initiate CR showers. The calorimeter (CAL) [7] then samples the shower using 20 alternating layers of tungsten plates and layers of ribbons of scintillating fibers. The scintillation light from the ribbons is guided to the instrument's light sensitive hybrid-photodiodes (HPDs), which convert the light signal to electrical pulses. The pulses are then integrated and digitized into ADC counts. The Boronated Scintillator Detector (BSD) [8] is designed to provide additional rejection power to electron/proton discrimination. It uses a slab of EJ-200 plastic scintillator doped with boron, which can absorb thermalized neutrons from the hadronic showers. The BSD is equipped with 2 early light photomultiplier tubes (PMTs) and 16 late light PMTs. The early light PMTs act as a self-trigger when they are activated by the scintillation light generated by the shower and the late light PMTs integrate light signals up to 4.9 μs after the shower is detected.

2.2 Determining the CAL energy scale

During its operation, ISS-CREAM collected over 5×10^7 events, among which $< 0.1\%$ have enough response in the CAL for energy reconstruction. This deficit in the dataset quantity is confirmed with a trained deep learning model that identifies CR showers [9]. Visual scans on selected events were also conducted to validate this result. A preliminary differential energy spectrum generated from the ISS-CREAM dataset appears to be orders of magnitude lower than the values reported by other experiments. This can be explained by either a lower than expected efficiency or an underestimate of the energy measured by the CAL due to an inaccurate calibration. Investigations of the ISS-CREAM efficiency is still ongoing, but we have not yet found any evidence of a specific

inefficiency that could account for this tension.

The CAL energy scale is not well defined absolutely. In fact, there was no pre-launch end-to-end calibration made of the ISS-CREAM CAL, partly owing to a compressed time schedule for instrument delivery for rocket launch. [10] has reported CAL calibration results when a copy of the CAL unit was studied using electron and pion beams at CERN. However, the ISS-CREAM CAL uses a different set of electronics which was not used in CERN beam calibrations. Only an indirect connection between these two sets of electronics is determined, based on charge gain measurements, when ADC response was mapped out as a function of a certain amount of charge in DAC units generated by the calibration boards. However, the size of a DAC unit is not known a priori, so this derivation includes some unvalidated assumptions, could be the source of uncertainties in the energy scale. In addition, there were mechanical modifications made to the detector after the accelerator test, which includes but is not limited to changing the HPDs that mates with fiber bundles, which could also have effected the calibration.

An attempt to calibrate the CAL ribbon response using non-interacting Fe nuclei was made with on-orbit data. It was estimated that an average of about 16 MeV energy is deposited in a ribbon if a non-interacting Fe nucleus traverses it. This amount of energy should pass the data sparsification process of the CAL, where ribbons with signals lower than a given threshold are removed to reduce the noise. The level of sparsification programmed on orbit was 20 ADC most of the time during ISS-CREAM operations, which corresponds to about 9 MeV based on the expected conversion factors on launch. Since ISS-CREAM is equipped with a low-energy trigger based on the TCD/BCD, it is possible that non-interacting Fe could be captured and recorded by the instrument's data acquisition system, which could then be used to find the conversion between ribbon signals in ADC and energy deposition in MeV. However, no such events were ever found. This dearth could be explained by a higher energy scale, i.e. where a given ADC signal corresponds to a higher energy deposition in MeV than initially thought. Consequently, the threshold of sparsification would be higher than the assumed value and any non-interacting particles would become invisible to the CAL.

3. CAL calibration using the BSD

3.1 Motivation and overview

The BSD was originally designed to provide electron/proton separation. However, since the BSD is using a monolithic piece of scintillator, it captures the tail of a CR-induced shower and collects the associated energy deposition. The ISS-CREAM BSD was calibrated using electron and pion beams in 2012 and an analysis of the late PMT signals shows good agreement with predictions from detailed GEANT4-based Monte Carlo (MC) simulations [11]. It was also discovered that the late signal was dominated by delayed fluorescence light and that the ratio between the fluorescence light integrated over the late window and the prompt light from the shower integrated over the early window is a fixed value. In addition, it was confirmed in [12] that the response of the late light PMT stays linear up to its full dynamic range. As we will demonstrate, it is possible to use the late-signal in the BSD PMTs to estimate the shower energy and this correlates well with the energy deposition in the CAL, enabling the BSD to be used for a shower energy measurement.

There are some uncertainties associated with the BSD signals. About one month after the launch

of ISS-CREAM, 4 of the 16 late light PMTs and 1 of the 2 early light PMTs failed permanently. The full reason behind this failure remains unknown but it is suspected that a fast ramping of a high voltage supply after an exit of the South Atlantic Anomaly could have been the cause. It was then decided to reduce the operating voltage of both early and late PMTs from 1200 V to 1050 V, after which the BSD remained stable and there were no further failures for the remainder of on orbit operations. As a result, the measured gain values of the PMTs need to be adjusted to account for the different operating voltage, which is a source of uncertainty. In addition, the integration window of late PMTs extends up to 4.9 μs after the shower, which surely captures some background radiation in the space environment and adds to the uncertainty. We attempt to solve this problem with an overall 'goodness of fit' test between the MC and ISS-CREAM data.

3.2 Processing the BSD signal

The time dependence of the gains of the PMTs was calibrated using on-board LED sources that flashed periodically (every 6 hours) at a fixed amount of brightness. The gains of the PMTs were observed to remain quite stable, with a correction introduced as a linear function of time with a small slope. This correction is applied after pedestal subtraction where the pedestal is determined daily using the real time data. Each PMT has two output ranges, low and high, which are stitched into one continuous signal in ADC units. The ADC signals are then converted to minimum-ionizing particle (MIP) equivalent signals, with a conversion based on lab measurements using ground muons before the integration of the BSD into ISS-CREAM.

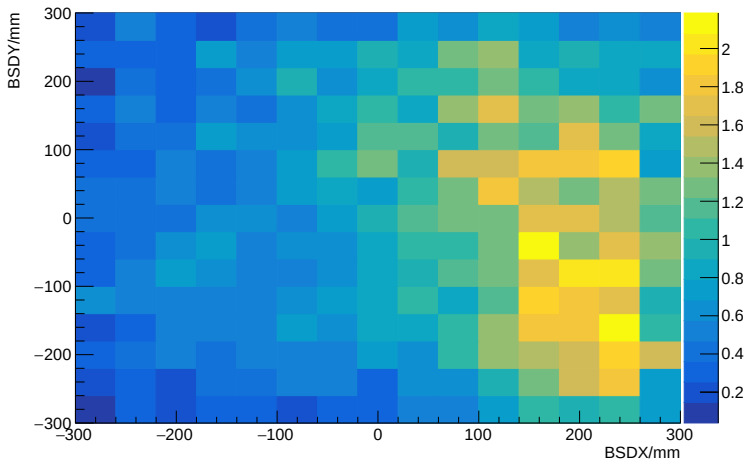

Fig. 1: Position dependence of PMT signals is shown using one of the PMT channels as an example. This PMT is located at the bottom right corner in this view, where the brighter (yellow) signals near it are readily apparent.

Since the measurement of PMT gains using ground muons was made when muons were incident at the center of the scintillator, further corrections of the signal are needed to account for the shower impact location on the scintillator. Maps of weighted signals based on hit locations on the BSD for each PMT were made using a carefully selected ISS-CREAM dataset which includes

CR events with clear charge identification and having tracks contained within the instrument. Fig.1 shows an example for one PMT, which is located near one corner of the BSD. The scintillator area is divided into 15×15 bins and the value in each bin corresponds to the average signal of that PMT for the events whose reconstructed tracks go through the area defined by that bin. The map is normalized to its center bin, which reflects the fact that no corrections will be needed should the hit go through the center. It can be seen in Fig.1 that there is a clear dependence on the hit location of the CR-induced shower—a closer hit to the PMT causes a higher signal. The signals in each event are thus normalized to correct for position dependence in the BSD. In the end, the BSD late signal is calculated as the average of signals in all 12 working late PMTs.

3.3 Calibration of the CAL

We select CR events with clear charge identification in the SCD and having tracks well contained inside the whole instrument as our calibration data sample. The tracking method used in this study is based on the combined information from the TCD, the top layer of the SCD, and the CAL. We select elements Z >= 6 (Carbon and higher) for the reconstructed events as these have the clearest tracks and the best reconstruction in the instrument. The signals in the SCD for high charges is above the common noise level so the top layer of the SCD provides reliable charge identification without undue contamination by back-scattered particles or noise pixels. The MC events go through the same selection process to ensure consistency of this study.

The left of Fig.2 shows profile histograms made by plotting CAL energy deposition against

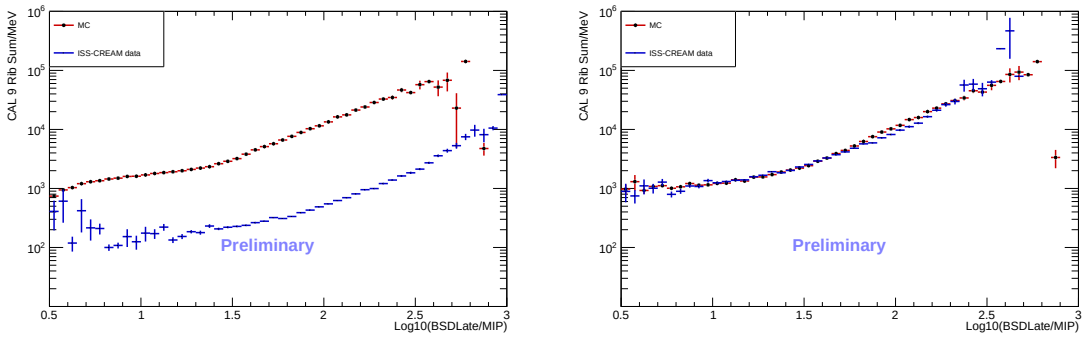

Fig. 2: Left: distribution of the CAL nine ribbon sum signal versus BSD late signal, without any scaling. Right: ISS-CREAM CAL signal rescaled by a factor of 6 after applying appropriate BSD scaling.

BSD late signal where blue stands for the ISS-CREAM data and red stands for the MC. The CAL energy deposition is calculated as the sum of nine ribbons of each layer where the center ribbon is found from the reconstructed track. It can be seen that the BSD signal is positively correlated to the CAL energy deposition. However, the MC clearly predicts a much higher energy deposition in the CAL for the same BSD signal than what is recorded in ISS-CREAM data. This tension between MC and ISS-CREAM data can be resolved by scaling up the MeV-to-ADC conversion factor of the ISS-CREAM event reconstruction, which is equivalent to bringing up the blue curve in the left figure. One subtlety that comes with this scaling is that the CAL response in MC needs to be sparsified according to the energy scale. For example, rescaling by a factor of 2 will remove

ribbons with signals smaller than 18 MeV instead of the assumed 9 MeV. As a result, the shape of the MC histogram may also change accordingly. The best result after scaling the CAL by a factor of 6 is shown in the right panel of Fig.2. Note that for a better agreement between MC and data, we do have to apply a scaling of the BSD signal as well, allowable due to the gain uncertainties described in Section 3.1 above. However, only scaling the BSD obviously wouldn't achieve this level of agreement.

To further justify our choice of the scaling factors, we conducted a parameter scan where

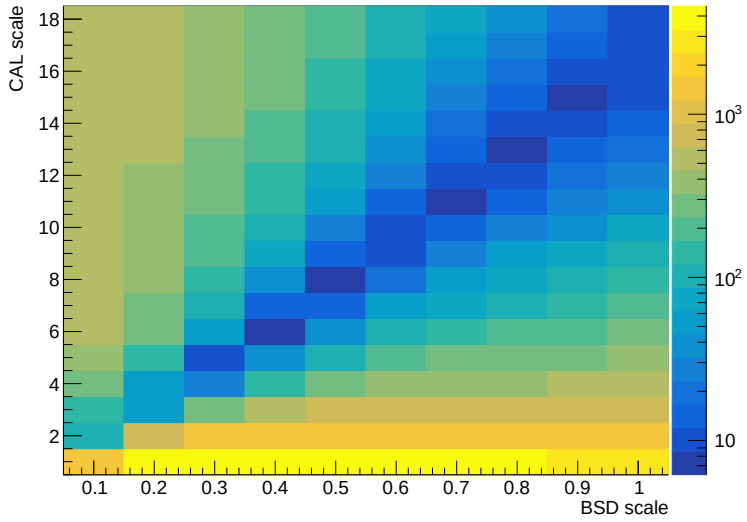

Fig. 3: The parameter space defined with a horizontal (BSD) scale and vertical (CAL) scale. The values in each bin are calculated based on a χ^2 statistic. Lower values are preferred.

we treat BSD and CAL scaling factors as free parameters. A BSD scaling parameter was varied between 0.1 to 1 in steps of 0.1 and a CAL scaling parameter was varied between 1 to 18 in steps of 1. For every set of scaling parameters, a χ^2 test statistic was calculated to evaluate the 'goodness of fit' between MC and ISS-CREAM data. Fig.3 shows the scanned parameter space where the χ^2 is reflected in the value of the bin. The size of the bins is the same as the step of the scan. The preferred region in the parameter space is along a diagonal line. The best match obtained is for a BSD scaling factor of 0.4 and a CAL scaling factor of 6, with a χ^2 value of 5.39 for 40 degrees of freedom. We plan to do further analysis with a finer scaling parameter in the preferred region and we will determine the region of confidence in the parameter space.

4. Conclusion

We described some difficulties encountered in analyzing the ISS-CREAM data, and in particular we identified a possible problem with the CAL energy determination. We used the BSD and on-orbit data to try and calibrate the CAL energy scale. The results are very promising and we believe further analysis will enable us to have a good calibration and understand the energy deposition in the CAL ribbons. Introduction of scaling factors to correct for this effect will help towards the final production of elemental spectra from ISS-CREAM data.

Acknowledgments

This work was supported in the U.S. by NASA grants NNX17AB43G, NNX17AB42G, and their predecessor grants, as well as by directed RTOP funds to NASA GSFC. The authors also thank M. Geske, Penn State, for contributions to the BSD, and K. Wallace at Northern Kentucky University for contributions to Monte Carlo simulations. We also recognize the contributions of past CREAM and ISS-CREAM collaborators.

References

[1] J. R. Hörandel, *Models of the knee in the energy spectrum of cosmic rays*, *Astroparticle Physics* **21** (2004) 241.

[2] A. Kounine, *The alpha magnetic spectrometer on the international space station*, *International Journal of Modern Physics E* **21** (2012) 1230005.

[3] S. Torii, *The CALorimetric Electron Telescope (CALET): a High-Energy Astroparticle Physics Observatory on the International Space Stati*, *PoS* **ICRC2015** (2016) 581.

[4] J. Chang, G. Ambrosi, Q. An, R. Asfandiyarov, P. Azzarello, P. Bernardini et al., *The DArk Matter Particle Explorer mission*, *Astroparticle Physics* **95** (2017) 6.

[5] J. Lee, Y. Amare, T. Anderson, D. Angelaszek, N. Anthony, K. Cheryian et al., *The ISS-CREAM Silicon Charge Detector for identification of the charge of cosmic rays up to $Z = 26$: Design, fabrication and ground-test performance*, *Astroparticle Physics* **112** (2019) 8.

[6] Y. S. Hwang, H. J. Kim, T. Anderson, D. Angelaszek, M. Copley, S. Coutu et al., *Construction and testing of a Top Counting Detector and a Bottom Counting Detector for the Cosmic Ray Energetics And Mass experiment on the International Space Station*, *Journal of Instrumentation* **10** (2015) P07018.

[7] K. C. Kim, ISS-CREAM Collaboration, Y. Amare, D. Angelaszek, N. Anthony, G. H. Choi et al., *On-orbit Performance of the ISS-CREAM Calorimeter*, in *Proceedings of 36th International Cosmic Ray Conference — PoS(ICRC2019)*, (Madison, WI, U.S.A.), p. 088, Sissa Medialab, July, 2019, DOI.

[8] Y. Amare, T. Anderson, D. Angelaszek, N. Anthony, K. Cheryian, G. H. Choi et al., *The boronated scintillator detector of the ISS-CREAM experiment*, *Nuclear Instruments and Methods in Physics Research Section A: Accelerators, Spectrometers, Detectors and Associated Equipment* **943** (2019) 162413.

[9] M. Yu, *Poster 476: Machine learning applications on event reconstruction and identification for iss-cream*, in *(ICRC2021)*.

[10] H. G. Zhang, D. Angelaszek, M. Copley, J. H. Han, H. G. Huh, Y. S. Hwang et al., *Performance of the ISS-CREAM calorimeter in a calibration beam test*, *Astroparticle Physics* **130** (2021) 102583.

[11] S. Nutter, Y. Amare, T. Anderson, D. Angelaszek, N. Anthony, k. Cheryian et al., *Measurement of delayed fluorescence in plastic scintillator from 1 to 10 μs*, *Nuclear Instruments and Methods in Physics Research Section A: Accelerators, Spectrometers, Detectors and Associated Equipment* **942** (2019) 162368.

[12] T. Anderson, Y. Chen, S. Coutu, S. Im, T. LaBree, J. T. Link et al., *Gated-Dynode photomultiplier tube assembly for the boronated scintillator detector of the ISS-CREAM experiment*, *Nuclear Instruments and Methods in Physics Research Section A: Accelerators, Spectrometers, Detectors and Associated Equipment* **942** (2019) 162343.